*Proceedings of MARTEC 2010*
*The International Conference on Marine Technology*
*11-12 December 2010, BUET, Dhaka, Bangladesh*

# A STUDY ON NUMERICAL ANALYSIS OF UNSTEADY FLOW OVER TWO DIMENSIONAL HYDROFOILS

**N. Mostafa[1], M. M. Karim[2], and M. M. A. Sarker[3]**

[1]Graduate School of Environment and Information Science, Yokohama National University, Yokohama, Japan.
E-mail: mostafa_nur@yahoo.com

[2]Department of Naval Architecture and Marine Engineering, BUET, Dhaka, Bangladesh
E-mail: mmkarim@name.buet.ac.bd

[3]Department of Mathematics, BUET, Dhaka, Bangladesh
E-mail: masarker@math.buet.ac.bd

## ABSTRACT

*The time dependent characteristics performance of cavitating flow around CAV-2003 hydrofoil has been simulated using pressure-based finite volume method. A bubble dynamics cavitation model is used to investigate the unsteady behavior of cavitating flow and describe the generation and evaporation of vapor phase. For choosing the turbulence model and mesh size a non cavitating study is conducted. The cavitating study presents an unsteady behavior of the partial cavity attached to the foil at different time steps in the case of σ=0.8. Moreover, this study is focused on cavitation inception, the shape and general behavior of sheet cavitation, lift and drag forces for different cavitation numbers.*

**Key words**: Cavitation, CAV2003 hydrofoil, finite volume method, k-ε turbulence model, unsteady flow.

## 1. INTRODUCTION

Cavitation in hydraulic machines causes different problems like vibration, increase in hydrodynamic drag, pressure pulsation, and change in flow kinematics, noise and erosion of solid surface. Most of these problems are related to transient behavior of cavitation structure. Cavitation erosion is strongly related to unsteady fluctuations of the cavitation zone. Hence a study of unsteady cavitation behavior is essential for a good prediction of the problem. To investigate cavitation phenomena and validate numerical procedures, a number of investigations were performed in the past [1, 4, 8, 9]. In the last decade various methods for numerical simulation of cavitating flow were developed. Most of the studies treat the two phase flow as a single vapor-liquid phase mixture flow. The evaporation and condensation can be modeled with different source terms that are usually derived from the Rayleigh-Plesset bubble dynamics equation.

Recently different authors proposed to consider a transport equation model for the void ratio, with vaporization/condensation source terms to control the mass transfer between two phases [10]. This method has the advantage that it can take into account the time influence on the mass transfer phenomena through empirical laws for the source term. It also avoids using quantities like bubble number density and initial bubble diameter. The other way to model cavitation process is by the so called barotropic state law that links the density of vapor-liquid mixture to the local static pressure.

A cavitation model, based on bubble dynamics equation [10] is used for computation of cavitating flows. The non-cavitating operation as well as influence of mesh and turbulence model, mainly by comparing the values of lift and drag are studied in the previous paper of the author [5]. Now two cavitating conditions are separately analyzed, i.e., σ=0.8 where an unsteady partial cavitating behavior is obtained and σ=0.4 where a supercavitating flow is observed. Cavitating flow at different cavitation numbers is analyzed and finally an unsteady partial cavitating behavior at σ=0.8 is observed at different time steps.

## 2. NUMERICAL SIMULATION

The numerical model uses an implicit finite volume method associated with multiphase and cavitation model. For numerical simulation of cavitating flow, a bubble dynamics cavitation model is used to describe the cavity formation. The RNG k-ε turbulence model with enhanced wall treatment is used as a turbulence model. The Reynolds number ($Re=5.9\times10^5$) based on chord length is used .The corresponding y+ is 5-15. A second order central scheme is used for discretization for space except for the convective terms. The convective term in the momentum equation is

discretized by the QUICK scheme for non cavitating flow and second order implicit scheme is used for cavitating problem. Pressure based solver SIMPLE is used as the velocity pressure–coupling algorithm

## 3. MULTIPHASE MODEL

A single fluid (mixture model) approach is used. The mass and momentum conservation equations together with the transport equation and the equation of the turbulence model from the set of equations from which fluid density (which is the function of the vapor mass fraction $f_v$) is computed. The $\rho_m - f_v$ (mixture density-vapor mass fraction) relation is [2]:

$$\frac{1}{\rho_m} = \frac{f_v}{\rho_v} - \frac{1-f_v}{\rho_l} \tag{1}$$

The volume fraction of the vapor phase $(\alpha_v)$ is related to the mass fraction of the vapor phase with:

$$\alpha_v = f_v \frac{\rho_m}{\rho_v} \tag{2}$$

The mass conservation equation for the mixture is:

$$\frac{\partial}{\partial t}(\rho_m) + \nabla.(\rho_m \vec{v}_m) = 0 \tag{3}$$

The momentum conservation equation for the mixture is

$$\frac{\partial}{\partial t}(\rho_m \vec{v}_m) + \nabla.(\rho_m \vec{v}_m \vec{v}_m) = -\nabla p + \nabla.\left[\mu_m\left(\nabla \vec{v}_m + \nabla \vec{v}_m{}^T\right)\right] + \rho m \vec{g} + \vec{F} \tag{4}$$

And the transport equation for the vapor is:

$$\frac{\partial}{\partial t}(\rho_m f_v) + \nabla.(\rho_m \vec{v}_m f_v) = R_e - R_c \tag{5}$$

## 4. CAVITATING MODEL

The working fluid is assumed mixture of liquid, liquid vapor and noncondensible gas. Source terms $R_e$ and $R_c$ define as vapor generation (liquid evaporation) and vapor condensation, respectively. The source terms can be expressed as [7].

$$R_e = C_e \frac{\sqrt{k}}{\gamma} \rho_l \rho_v \sqrt{\frac{2}{3}\frac{p_v - p}{\rho_l}\left(1 - f_v - f_g\right)},$$

when $p < p_v$ (6)

$$R_c = C_e \frac{\sqrt{k}}{\gamma} \rho_l \rho_v \sqrt{\frac{2}{3}\frac{p_v - p}{\rho_l}} f_v,$$

when $p > p_v$ (7)

where $C_e$ and $C_c$ are empirical constants, and k is the local kinetic energy, $\gamma$ is the surface tension, $f_v$ is vapor mass fraction and $f_g$ is mass fraction of noncondensable (dissolved) gases. Values of $C_e$ and $C_c$ are 0.02 and 0.01 respectively.

## 5. GEOMETRY AND COMPUTATIONAL DOMAIN

The section of the hydrofoil is presented in Figure 1 which shows a schematic view of the CAV2003 hydrofoil geometry. The hydrofoil is placed at an angle of attack $7^0$. The equation of the upper surface of the symmetric foil geometry is provided as

$$\frac{y}{c} = a_0\sqrt{\frac{x}{c}} + a_1\left(\frac{x}{c}\right) + a_2\left(\frac{x}{c}\right)^2 + a_3\left(\frac{x}{c}\right)^3 + a_4\left(\frac{x}{c}\right)^4 \tag{8}$$

where $a_0 = 0.11858$, $a_1 = -0.02972$, $a_2 = 0.00593$, $a_3 = -0.07272$, $a_4 = -0.002207$

$\bar{y} = y/c$ and $\bar{x} = x/c$ is the dimensionless coordinate along the chord line. The flow field around the hydrofoil is modeled in two dimensions. The flow from left to right with the hydrofoil of chord length $c = 0.1$ m submersed in an incompressible fluid is considered. The hydrofoil is located at the middle of a channel of length 10c and height 4c. Figure 1 shows the total 2D computational domain and boundary conditions. The inlet boundary condition is specified velocity inlet with a constant velocity profile which is 6 m/s. Upper and lower boundaries are slip walls, i.e., symmetry boundary condition. The outlet uses a constant pressure boundary condition. The foil itself is a no-slip wall, i.e., u = 0, v = 0 at the foil surface.

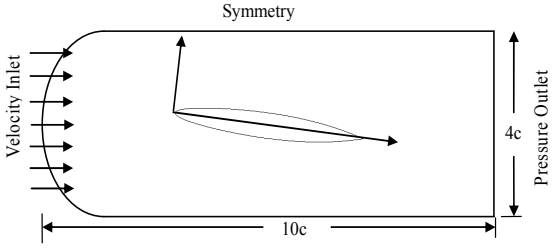


Figure 1. Schematic diagram of the flow field around CAV2003 hydrofoil with boundary condition.

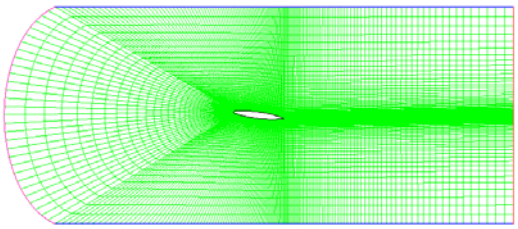

Figure 2. The overall view of grid lines in mesh.

## 6. CAVITATING ANALYSIS

This section presents results computed for the typical cavitation numbers σ=0.8 and σ=0.4. For simulation the convergence criterion is determined by observing the evaluation of different flow parameters (velocity magnitude at inlet, static pressure behind the hydrofoil) in the computational domain. For computation, each value of residual is taken as $10^{-4}$. Time step size has a great influence on simulation of cavitating flow. Different time step values are tested, eventually the time step for unsteady computation is set to $5\times10^{-5}$ and approximately 30 iterations per time step are needed to obtain a converged solution. To predict the behavior of the cavitating flow for the values of cavitation number σ = 0.8 and σ = 0.4, we first present comparisons of the computed time-averaged lift and drag coefficient for cavitating flow with Pouffary et al. [7], Courtier -Delgosha et al. [1], Kawamura et al, [6] and Yoshinori et al. [11]. Table 1 shows that the lift coefficient and the drag coefficient are in good agreement with published results.

Table 1. Comparison of time-averaged lift and drag coefficient at cavitation numbers σ = 0.8 and σ = 0.4

| | σ=0.8 | | σ=0.4 | |
|---|---|---|---|---|
| | $\overline{C}_L$ | $\overline{C}_D$ | $\overline{C}_L$ | $\overline{C}_D$ |
| Present | 0.44 | 0.077 | 0.214 | 0.076 |
| Pouffary | 0.456 | 0.0783 | 0.291 | 0.086 |
| Courtier-Delgosha | 0.450 | 0.0700 | 0.200 | 0.065 |
| Kawamura | 0.399 | 0.047 | 0.187 | 0.063 |
| Yoshinori | 0.417 | 0.0638 | 0.160 | 0.056 |

The time average values of lift and drag coefficients calculated by present method for the cavitation number σ = 0.8 are very close to the numerical result of Pouffary et al. [7]. However, the results show little discrepancy at cavitation number σ = 0.4. This discrepancy may be attributed due to the fact that different researchers used different turbulence models. The comparisons of the pressure distribution on the foil surface for σ=0.4 is shown in Figure 3. It compares the present result with the result of Kawamura et al. [6]. There exists a good agreement but some difference in magnitude may be due to the k-ω turbulence model used by Kawamura et. al. [6]. The difference in pressure distribution on the face side is found very small. Similar comparison is shown in Figure 3 for σ=0.8. The time history of the lift and drag coefficients computed by mixture model at σ = 0.8 and σ = 0.4 are shown in Figure 4 respectively. The characteristics of the curve of lift and drag coefficients are almost similar. The contours of pressure coefficient and vapor volume fraction for cavitation numbers σ=0.8 and 0.4 are shown in Figure 5. These contours show the expansion of cavity and their sizes for different cavitation numbers. At σ=0.8 the half of the hydrofoil is covered with vapor and at σ=0.4 the back surface is covered with vapor and it decreases with the increase in cavitation number and cavity length become shorter.

Figure 6 and Figure 7 show the instantaneous field of pressure distribution and vapor volume fraction respectively computed for five time levels t=0.47s, 0.49s, 0.52s, 0.55s and 0.57s in the case of σ=0.8. These figures clearly show the creation and collapsing of cavity over the hydrofoil surface.

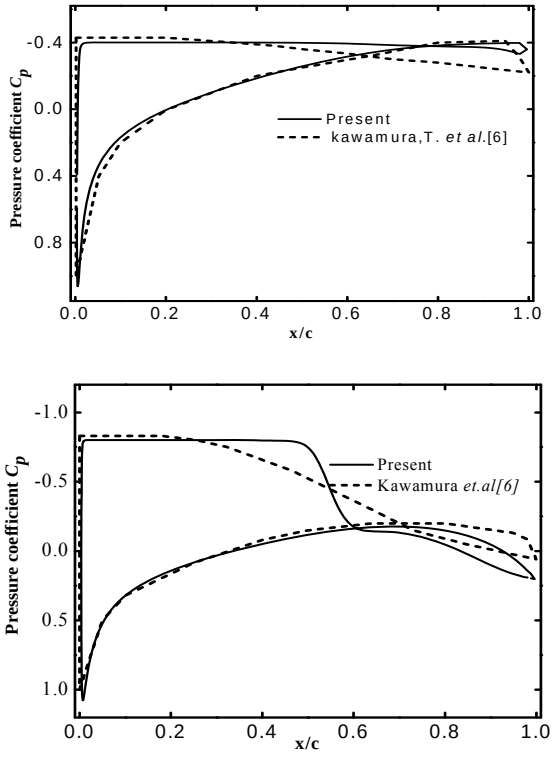


Figure 3. Comparison of the pressure coefficient on the foil surface at σ =0.4 and σ =0.8 respectively.

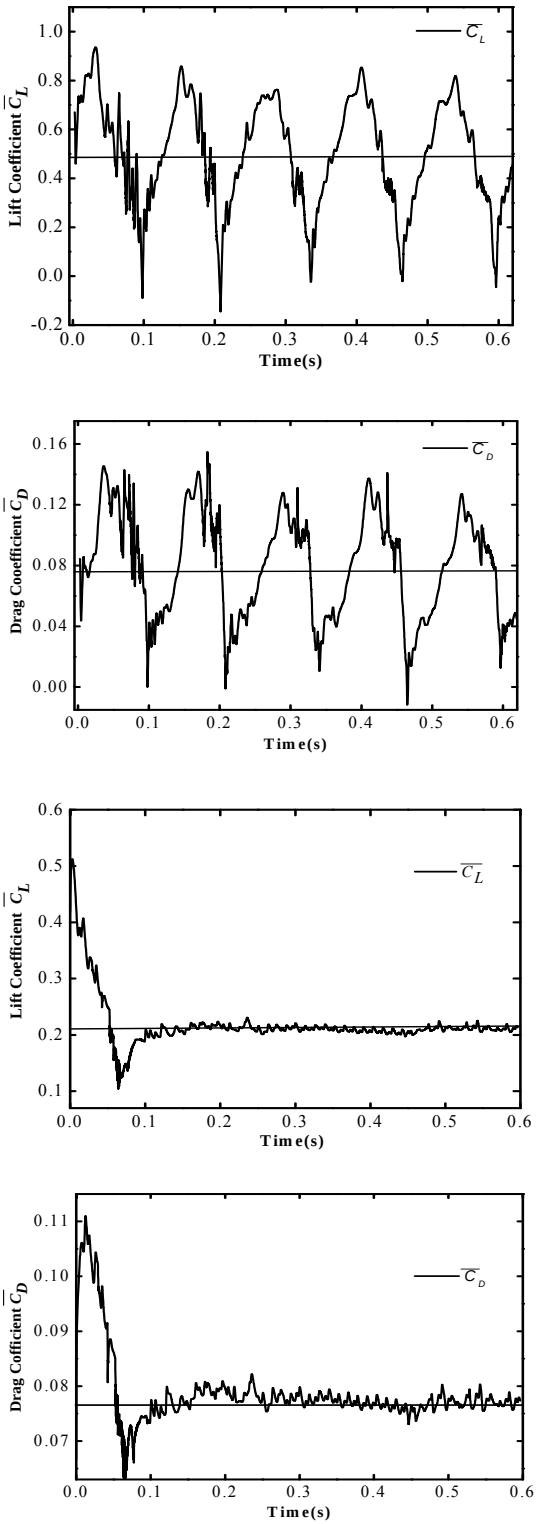


Figure 4. Time history of lift coefficient and drag coefficient at σ=0.8 and σ=0.4 respectively.

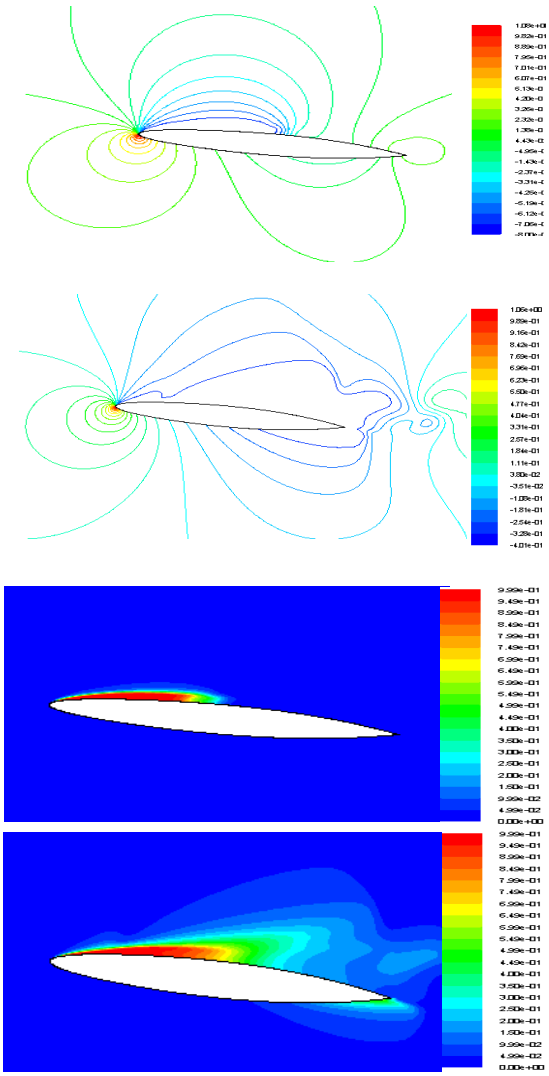

Figure 5. Contour of pressure coeffcient and contour of vapor volume fraction at σ=0.8 and σ=0.4

It is observed that the length of sheet cavity grows gradually until the cavity trailing edge almost reaches the end of a foil, and then reverse flow emerges near the foil trailing edge. The reverse flow propagates towards the leading edge along the back surface of edge foil causing collapse of the sheet cavity. Table 2 shows the summary of the cavitation parameters where $\bar{l}_{\max}$ , $\bar{t}_{\max}$ and $\bar{l}_{t\ \max}$ are maximum cavity length, maximum cavity thickness and the position of maximum cavity thickness respectively. As the cavitation number decreases, the maximum cavity length and maximum cavity thickness increase. On the other hand the position of maximum cavity thickness is almost constant at 75% of the maximum cavity length except for σ = 0.4. In the case of σ = 0.4, a super cavitating flow fully develops and the cavitation also appears on the pressure side near the

trailing edge. It is also seen that the time-averaged lift coefficient decreases and the time-averaged drag coefficient increases as the cavitation number decreases. However, after $\sigma$ =0.9, it decreases slightly.

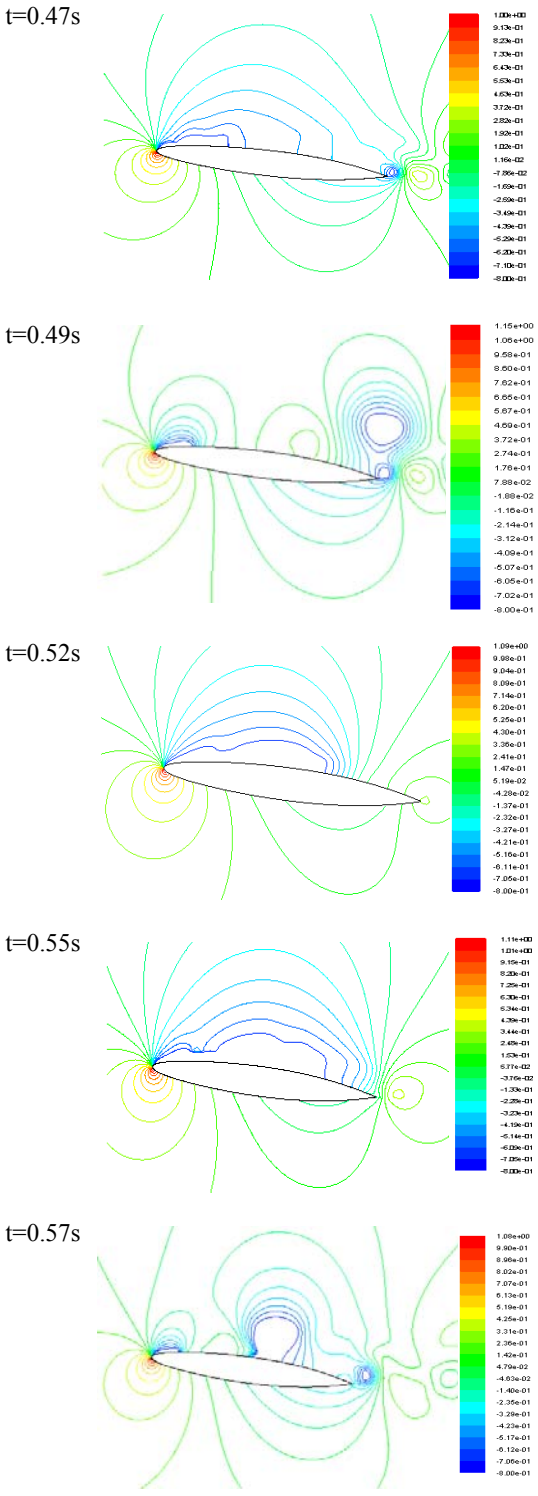


Figure 6. countour of the presure coefficient at different times in the case of σ=0.8

Figure 8 shows the variation of maximum cavity length and maximum cavity thickness with the cavitation number. The idea of change pattern can be obtained from this figure.

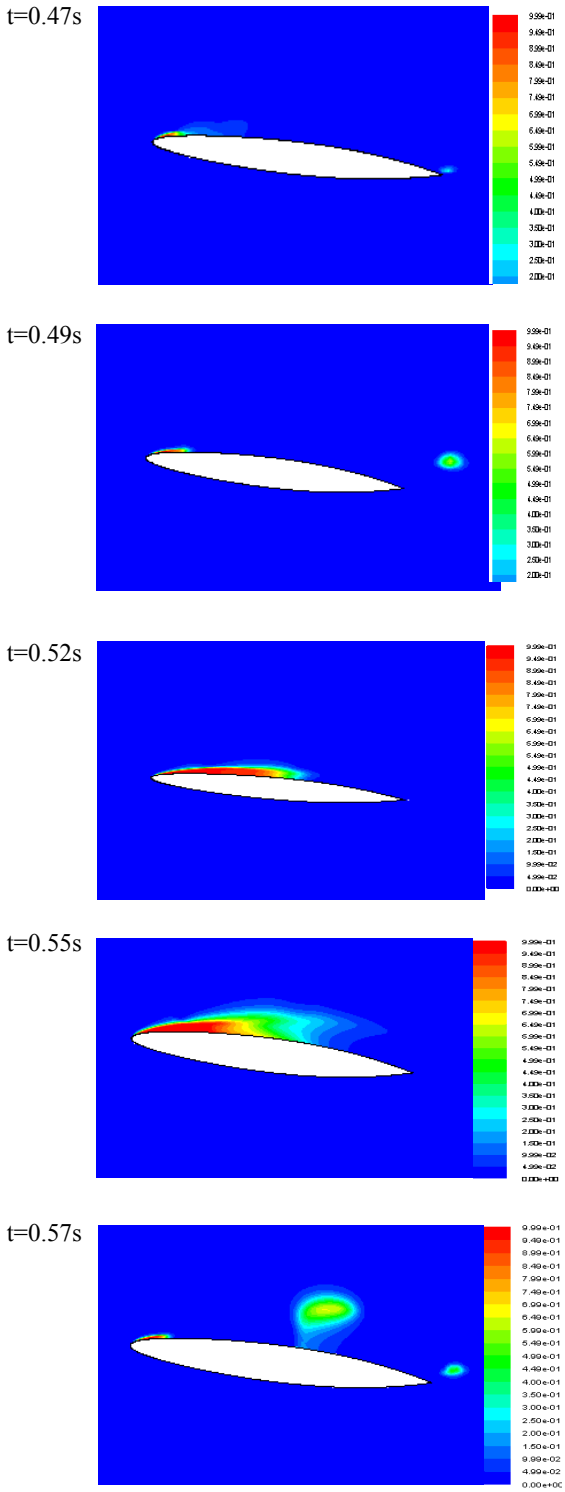


Figure 7. Countour of the volume fraction at different times in the case of σ=0.8

Table 2. Comparisons of time-averaged lift and drag coefficient at cavitation numbers σ = 0.8 and σ = 0.4

| σ | $\bar{l}_{\max}$ | $\bar{t}_{\max}$ | $\bar{l}_{t\ \max}$ | $\overline{C}_L$ | $\overline{C}_D$ |
|---|---|---|---|---|---|
| 3.5 | - | - | - | 0.667 | 0.024 |
| 1.5 | 0.098 | 0.0211 | 0.76 | 0.582 | 0.0378 |
| 1.2 | 0.16 | 0.0329 | 0.79 | 0.57 | 0.0425 |
| 1.1 | 0.21 | 0.0465 | 0.73 | 0.566 | 0.0446 |
| 1.0 | 0.25 | 0.047 | 0.73 | 0.560 | 0.0476 |
| 0.9 | 0.45 | 0.0772 | 0.78 | 0.51 | 0.0783 |
| 0.8 | 0.49 | 0.0784 | 0.71 | 0.44 | 0.077 |
| 0.4 | 1.00 | 0.28 | 0.66 | 0.214 | 0.0763 |

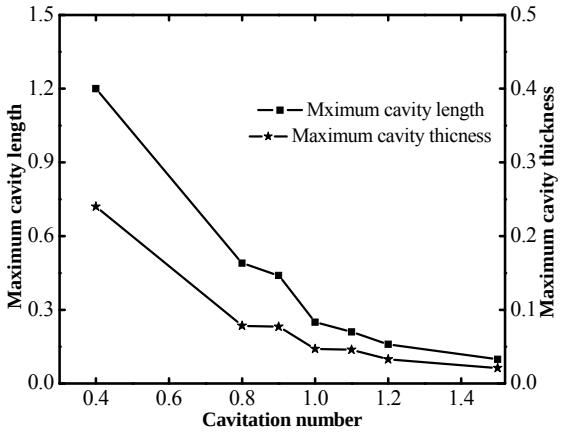


Figure 8. Plot for maximum cavity length and maximum cavity thickness versus cavitation number

## 7. CONCLUTION

Two-dimensional finite volume method has been applied to simulate in compressible flow around CAV2003 hydrofoil. For cavitation number σ=0.8, an unsteady partial cavitating behavior and for cavitation number σ=0.4, unsteady supercavitating behavior is simulated. In general, the results are very promising. The instantaneous pressure distribution and vapor volume fraction computed are shown at different time steps. Therefore, it is clearly understood that the length of the sheet cavity grows gradually towards the trailing edge and reverse flow emerge near the foil trailing edge and propagates towards the leading edge and causing the creation and collapsing of cavity over the hydrofoil surface. Finally, analysis is done for different cavitation numbers and the computed maximum cavity length and maximum cavity thickness show good correlation with cavitation numbers.

## REFERENCES

[1] Coutier-Delgosha, O. and Jacques A. A., "Numerical reduction of cavitating flow on a two–dimensional symmetrical hydrofoil with a single fluid model," *Fifth International Symposium on Cavitation (Cav2003),* Osaka, Japan, November 1-4, (2003).

[2] Dular, M., Bacher, R., Stoffel, B. and Širok, B. "Experimental evaluation of numerical simulation of cavitating flow around hydrofoil," *European Journal of Mechanics B/Fluids* 24, 522-538, (2005).

[3] Frobenius, M., Schilling, R., Bachert, R. and Stoffel, B., "Three-dimensional, unsteady cavitation effects on a single hydrofoil and in a radial pump – measurements and numerical simulations, Part two: Numerical simulation," *in: Proceedings of the Fifth International Symposium on Cavitation*, Osaka, Japan, (2003).

[4] Kubota, A., Hiroharu, A. and Yamaguchi, H., "A new modeling of cavitating flows, a numerical study of unsteady cavitation on a hydrofoil section," *J. Fluid Mech*. 240, 59–96, (1992).

[5] Karim, M. M., Mostafa, N. and Sarker, M. M. A., "Numerical prediction of unsteady cavitating flow around hydrofoil," *Proceeding of 16th Mathematical Conference of Bangladesh Mathematical Society*, 17-19 December, (2009).

[6] Kawamura, T. and Sakuda, M., "Comparison of bubble and sheet cavitation models for simulation of cavitation flow over a hydrofoil," *Fifth International Symposium on Cavitation (Cav2003),* Osaka, Japan, November 1-4, (2003).

[7] Pouffary, B., Fortes-Patela, R. and Reboud, J.L., "Numerical simulation of cavitating flow around a 2D hydrofoil: A barotropic approach," *Fifth International Symposium on Cavitation (Cav2003),* Osaka, Japan, November 1-4, (2003).

[8] Stutz, B. and Reboud, J. L, "Measurements within unsteady cavitation," *Exp. Fluids* 29, 545–552, (2002).

[9] Schnerr, G. H. and Sauer, J., "Physical and numerical modeling of unsteady cavitation dynamics," *in: 4th International Conference on Multiphase Flow,* ICMF-2001, New Orleans, USA, (2001).

[10] Singhal, A. K., Li, H., Atahavale, M. M. and Jiang, Y., "Mathematical basis and validation of the full cavitation model," *J. Fluids Eng*. 124, 617–624, (2002**).**

[11] Yoshinori S., Ichiro N. and Tosshiaki I., "Numerical analysis of unsteady vaporous cavitating flow around a hydrofoil," *Fifth International Symposium on Cavitation (Cav2003)*, Osaka, Japan, November 1-4, (2003).